



- Author(s)** Zdanowicz, Mariusz; Harra, Juha; Mäkelä, Jyrki M.; Heinonen, Esa; Ning, Tingyin; Kauranen, Martti; Genty, Goëry
- Title** Ordered multilayer silica-metal nanocomposites for second-order nonlinear optics
- Citation** Zdanowicz, Mariusz; Harra, Juha; Mäkelä, Jyrki M.; Heinonen, Esa; Ning, Tingyin; Kauranen, Martti; Genty, Goëry 2013. Ordered multilayer silica-metal nanocomposites for second-order nonlinear optics. Applied Physics Letters vol. 103, num. 25, 1-5.
- Year** 2013
- DOI** <http://dx.doi.org/10.1063/1.4852795>
- Version** Publisher's PDF
- URN** <http://URN.fi/URN:NBN:fi:ty-201409021421>
- Copyright** Copyright 2013 American Institute of Physics. This article may be downloaded for personal use only. Any other use requires prior permission of the author and the American Institute of Physics. The following article appeared in M. Zdanowicz et al., Appl. Phys. Lett. 103, 251907 (2013) and may be found at <http://dx.doi.org/10.1063/1.4852795>.

All material supplied via TUT DPub is protected by copyright and other intellectual property rights, and duplication or sale of all or part of any of the repository collections is not permitted, except that material may be duplicated by you for your research use or educational purposes in electronic or print form. You must obtain permission for any other use. Electronic or print copies may not be offered, whether for sale or otherwise to anyone who is not an authorized user.

Ordered multilayer silica-metal nanocomposites for second-order nonlinear optics

Mariusz Zdanowicz,^{1,a)} Juha Harra,^{1,b)} Jyrki M. Mäkelä,¹ Esa Heinonen,² Tingyin Ning,¹ Martti Kauranen,¹ and Goëry Genty¹

¹*Department of Physics, Tampere University of Technology, P.O. Box 692, FI-33101 Tampere, Finland*

²*Center of Microscopy and Nanotechnology, University of Oulu, P.O. Box 7150, FI-90014, Finland*

(Received 22 October 2013; accepted 6 December 2013; published online 18 December 2013)

We use aerosol synthesis to fabricate ordered metal-silica nanocomposites consisting of alternating layers of pure silica and silica nanoparticles decorated with silver nanodots. These multilayer structures preserve the narrow plasmon resonance of the nanodots even for high optical densities and allow second-harmonic generation due to spontaneous symmetry breaking arising from the interfaces between silica and nanoparticle layers. Our concept opens up perspectives for complex structures for advanced optical applications. © 2013 AIP Publishing LLC. [<http://dx.doi.org/10.1063/1.4852795>]

The optical responses of metal nanoparticles arise from the plasmonic oscillations of their conduction electrons. The resulting localized surface plasmon (LSP) resonances give rise to strong electromagnetic fields near the metal-dielectric interface. Such local-field enhancement has many attractive applications in biosensing,^{1,2} imaging,^{3,4} and solar cells.^{5,6} In addition, the plasmon resonances depend sensitively on the particle size,^{7,8} shape,^{9–12} as well as their dielectric environment, allowing broad tailorability of the resonances for a given application.

The local-field enhancement is particularly important for nonlinear optical effects, which scale with a high power of the field. Indeed, enhancement of third-order effects, with no particular symmetry constraints, has been demonstrated in bulk-type metal-dielectric nanocomposites.^{13,14} Second-order effects, such as second harmonic generation (SHG), on the other hand, require non-centrosymmetric samples, and their observation has so far been limited to surface geometries. Enhancement of SHG by rough metal surfaces was demonstrated early on in a traditional surface geometry where the incident beam is applied on the sample at oblique angle.¹⁵ More recently, lithographic arrays of non-centrosymmetric particles have been introduced as second-order metamaterials whose response can be accessed at normal incidence,^{16–19} but such samples are not easy to fabricate.

The nonlinear responses (both second and third-order) of a macroscopic sample can be enhanced by tuning the incident laser close to the plasmon resonance of the particles^{20,21} or by increasing the density of the particles. Unfortunately, the latter approach spoils the quality (shape and linewidth) of the resonances either due to agglomeration of particles, which gives rise to inhomogeneous broadening,^{22,23} or because of near field coupling.²⁴ An associated problem is the difficulty of fabricating bulk-type composite materials with the required non-centrosymmetry for second-order. For other types of materials, the organic ones in particular, the non-centrosymmetry can be induced afterwards by poling in

an electric field²⁵ or by using self-assembly, which in some cases gives rise to a non-centrosymmetric structure.²⁶ With regard to metal nanostructures, the focus has been on the plasmonic enhancement of the nonlinearity,²⁷ but no methods have been demonstrated for fabricating thick non-centrosymmetric structures.

Nanoparticle synthesis by aerosol techniques is fairly inexpensive, simple, highly versatile, and also scalable.^{28,29} Particles can be generated in a continuous process and deposited directly from the gas phase onto the desired substrate. Recently, aerosol techniques have been used to produce plasmonic metal nanoparticles from different materials and with various morphologies.^{23,30,31} In addition, the synthesized nanoparticles have been incorporated into multilayer polymer films in order to achieve for example magnetic and plasmonic functionalities.³² However, even though aerosol synthesized nanoparticles have been studied extensively using linear spectroscopy, their applicability in nonlinear optical materials remains to be explored.

In this Letter, we use aerosol techniques to fabricate ordered multilayer metal-silica nanocomposites with controllable linear and nonlinear optical responses. Our nanocomposites consist of alternating layers of silver-decorated silica particles and pure silica glass. The fabrication technique allows for precise control of the synthesis and deposition of the silver-decorated particles, thus preventing the formation of silver clusters and resulting in samples with reproducible optical properties. The shape of the plasmon resonance in the extinction spectrum of the ordered composites is perfectly maintained during the layer growth and its amplitude grows linearly as the number of layers increases. Significantly, we further show that symmetry is inherently broken due to interfaces between pure silica and a layer of decorated nanoparticles, resulting in spontaneous growth of a non-centrosymmetric structure and a SHG signal that increases with the number of layers. The SHG is dramatically larger than that observed from a single layer of decorated particles with equivalent thickness.

Silver-decorated silica nanoparticles (Fig. 1(a)) were synthesized in a continuous flow of nitrogen. The silica particles generated by chemical vapor synthesis from liquid tetraethyl orthosilicate (TEOS)³³ were subsequently sintered in

^{a)}Also at Transmission and Optical Technologies Department, National Institute of Telecommunications, Szachowa Str. 1, 04-894 Warsaw, Poland.; Electronic mail: mariusz.zdanowicz@tut.fi.

^{b)}M. Zdanowicz and J. Harra contributed equally to this work.

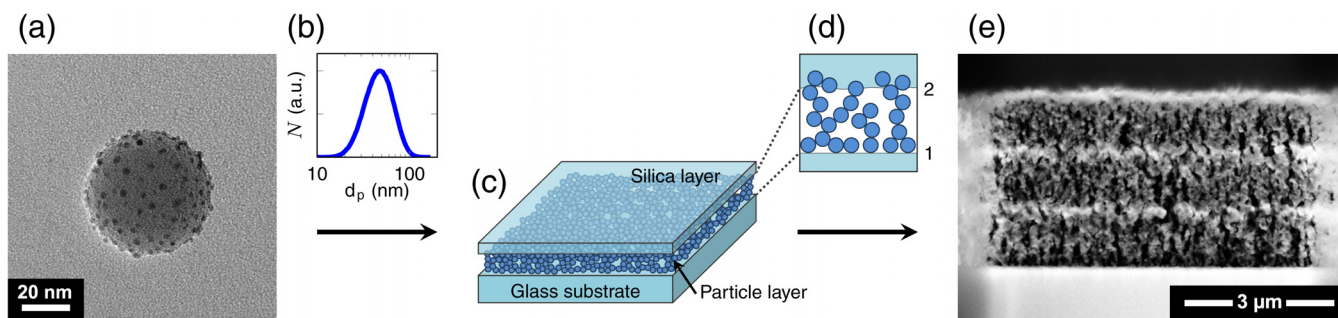


FIG. 1. (a) TEM image of a silver-decorated silica nanoparticle. (b) Size distribution of the silica particles (note the log scale in the horizontal axis). (c) Schematic image of one layer, which consist of a particle layer covered by a pure silica layer. (d) Schematic image of two neighboring interfaces explaining the symmetry breaking. (e) TEM image of the cross-section of a fabricated three-layer sample.

a tubular high-temperature furnace in order to obtain spherical carrier particles. Figure 1(b) shows the log-normal size distribution of the sintered silica particles, measured with a scanning mobility particle size (SMPS),³⁴ with a geometric mean diameter of 50 nm and a geometric standard deviation of 1.4. The silver decoration on the silica carrier particles was achieved by evaporation and subsequent condensation of silver from a small piece of bulk material.³¹ This resulted in the formation of silver nanodots with diameters of 1–2 nm. The synthesized silver-decorated silica particles were then deposited from the gas phase onto glass substrates (1 mm thick microscope glass slides) by electrostatic collection.³⁵ The circular particle collection area on the substrate had a diameter of 2 cm.

The thickness of the particle layer on the substrate depends on collection time. Here, the collection time was set to 30 min, corresponding to particle layer thickness of approximately $1\mu\text{m}$ with an estimated porosity of over 90%. This rough evaluation is based on the aerosol measurements (particle size and number concentration), particle collection parameters (gas flow rate, collection area and time) and realized layer thickness. Moreover, our estimation is consistent with previous reports of high porosity values for dry deposition of nanoparticles.³⁶ The layer of decorated nanoparticles was subsequently covered with a layer of pure silica using an electron-beam dielectric coater and with thickness, here approximately 200 nm, also determined by the deposition time (Fig. 1(c)). Repeating the particle deposition and coating processes multiple times and with identical deposition times allowed us to fabricate ordered multilayer nanocomposites whose linear and nonlinear optical properties can be controlled via the number of layers. Because the layer of silver-decorated particles is very porous, the silica coating penetrates it. However, the silica coating diffuses much less towards the bottom of the particle layer, and hence the overall symmetry of each layer is broken between the bottom and top interfaces (1 and 2, respectively, in Fig. 1(d)). Because each individual layer exhibits the same type of asymmetry the SHG response can grow significantly with the number of layers. In what follows, we use the term layer to refer to the combination of a single layer of decorated particles coated with a silica layer. Figure 1(e) shows a transmission electron microscope (TEM) image of the cross-section of a fabricated nanocomposite with three layers where the alternating layers of decorated nanoparticles and silica can be identified.

We first examined the linear optical properties of the fabricated samples. For this purpose, we measured their extinction spectra as a function of the number of layers with a high-sensitivity, high-resolution UV-Vis-NIR spectrophotometer (Shimadzu UV-3600). First, we clearly identify in each case the typical plasmon resonance of silver particles centered at around 370 nm (Fig. 2(a)) indicating the absence of silver clusters that would significantly broaden the resonance. Significantly, we also see how the magnitude of the extinction maximum grows linearly with the number of layers (see inset in Fig. 2(a)) and how the spectral location and width of the plasmon resonance remain unchanged with the number of layers. Oscillations visible for the wavelength

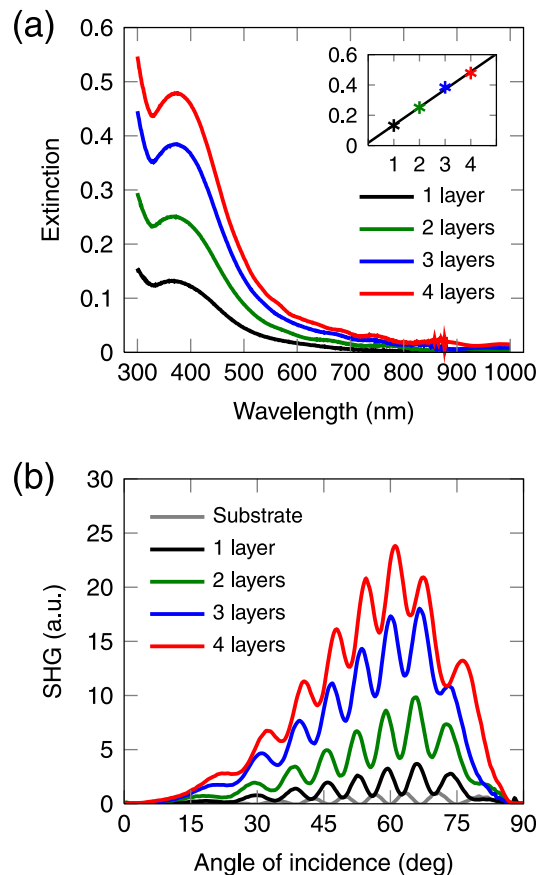


FIG. 2. (a) Extinction spectra of the multilayer nanocomposites. The inset shows the maximum extinction as a function of the number of layers. (b) Second-harmonic signal generated as a function of the angle of incidence.

TABLE I. Normalized SHG signals for different input-output polarization configurations.

$p_{in}-p_{out}$	$s_{in}-p_{out}$	$p_{in}-s_{out}$	$s_{in}-s_{out}$
1	8.9×10^{-2}	4.4×10^{-3}	0.7×10^{-3}

above 600 nm arise from weak Fabry-Perot effects within the active layers.

We then proceeded to investigate the second-order nonlinear response of the multilayer composites. The nonlinear response was characterized by measuring the SHG response as a function of the incidence angle in a Maker-fringe setup.^{37,38} The fundamental beam was derived from a Nd:YAG laser producing 70 ps pulses at 1 kHz repetition rate and with 1064 nm wavelength. A 25 cm focal-length lens was used to weakly focus the beam into a spot size of around 20 μm at the sample plane, leading to the generation of SHG radiation at the 532 nm wavelength. Any potential SHG from the laser itself was removed with a long-pass IR filter inserted before the sample. The fundamental beam was blocked after the sample with a combination of a short-pass filter and an interference filter (central wavelength 532 nm, bandwidth 10 nm). The transmitted SHG signal was detected by a photomultiplier tube and the polarization states of the fundamental and SHG beams were controlled with calcite Glan polarizers. The sample was mounted on a high precision rotation stage to detect the SHG as a function of the angle of incidence. The SHG signal was found to be a highly directional beam, thus verifying the coherent character of the process.

The measurements were performed for samples consisting of 1 to 4 layers, for various polarization configurations and the maximum SHG was observed for the input and output polarizations parallel to the plane of incidence ($p_{in}-p_{out}$ configuration, Table I). Very weak SHG signals for the $p_{in}-s_{out}$ and $s_{in}-s_{out}$ combinations suggest that the sample is isotropic in the plane of the sample as expected due to the fabrication process. In order to eliminate the possible influence of inhomogeneity in the sample plane, a series of measurements were conducted at ten different spatial locations on the samples. The SHG intensity was then averaged over all ten measurements. The results (Fig. 2(b)) show that the maximum of the SHG signal occurs for an incidence angle of

approximately 60°. Most importantly, the strength of the SHG signal increases with the number of layers in the sample. The Maker-fringes are also clearly observed and result from interference between the SHG signals arising from the back side of the 1 mm thick glass substrate. The thickness of any composite itself is much smaller than that of the substrate and their effect on the Maker-fringes cannot be resolved. The shift of the SHG signal maximum originates from the fact that the values of the susceptibility components for the active layers and the bottom surface of the substrate are different. As the active layer becomes thicker, its response becomes more important giving rise to changes in the fringe structure.

In order to evaluate the origin of the second-order response of the structures, we fabricated two additional control samples (see Fig. 3(a) for a schematic illustration). The first (CS1) consists of a single layer of silver-decorated particles coated with one layer of silica on top. Both layers were deposited so as to match the effective thicknesses of the respective layers in the four-layer sample. The other control sample (CS2), was prepared by depositing four layers of silica particles with no silver decoration. The collection time for the silica particles and the thickness of the deposited silica were identical to those of the four-layer sample with the silver decoration. The purpose of these two samples is two-fold: CS1 allows us to investigate the effect of structuring the samples into multiple layers whilst CS2 allows verifying the role of the silver particles in the nonlinear response.

We first compare in Fig. 3(b) the extinction spectra of the control samples and the four-layer sample. The linear response of the samples is seen to be essentially independent of the exact layer structure and only depends on the total silver and silica content. This can be understood from the fact that the only parameter that determines the overall extinction is the total amount of silver dots and silica and not the particular arrangement within the sample. This is an important result as it implies that any differences in the nonlinear response can be ascribed to the structuring of the samples into multiple layers. On the other hand, in the linear response of CS2 with no silver inclusions, we note, as expected, the absence of the plasmon resonance with an increase in the extinction for decreasing wavelengths consistent with typical silica absorption. These results clearly show that the extinction of the samples with silver-decorated particles is

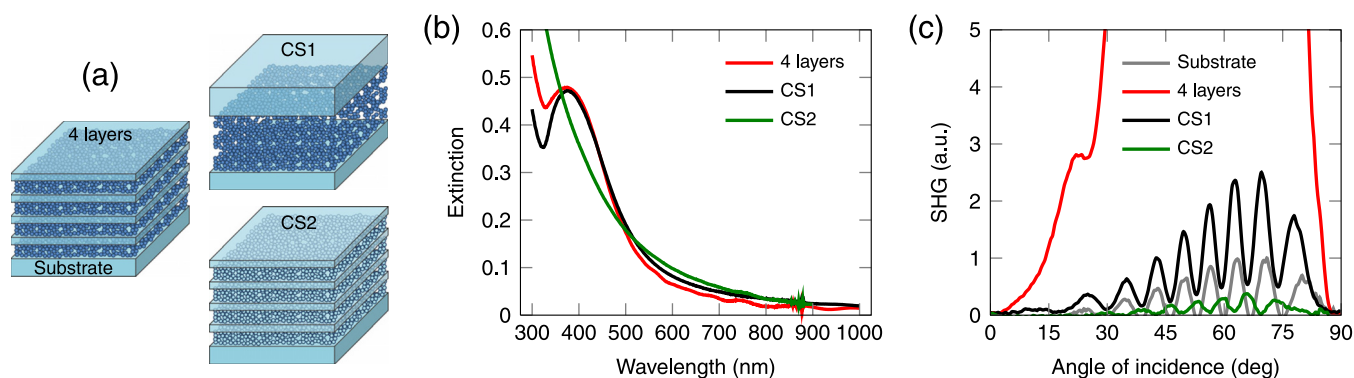


FIG. 3. (a) Schematic images of the multilayer nanocomposites and control samples. (b) Comparison of the extinction spectra between the four-layer sample and the control samples: CS1 with equivalent amount of metal and silica and CS2 with layers organized identically with four-layer structure, but without silver inclusions. (c) Comparison of the SH signal for the four-layer sample and the control samples CS1 and CS2.

dominated by the plasmon resonance as determined by the silver particle size and their total amount.

We subsequently performed the Maker-fringe experiments for the control samples under conditions identical to that of the multilayer composites. The results are presented in Fig. 3(c) along with the SHG intensity obtained from the four-layer structure and from the sole substrate. We first note that CS2 containing no decorated particles produces negligible SHG. In fact, the SHG signal from CS2 is even weaker than that from the substrate itself. On the other hand, CS1, which contains decorated particles, shows an increase in SHG compared to CS2 or the substrate, showing evidence of the importance of the silver nanoparticles in the SHG process. But most importantly, the SHG signal is more than order of magnitude weaker than that generated from the four-layer sample with the same quantity of silver. This is a truly remarkable result illustrating that (i) the multilayer structure plays a central role in enhancing SHG and (ii) SHG arises from the multiple coherent second-harmonic contributions induced by the symmetry-breaking arising from the differences between the top and bottom interfaces of each layer.

The SHG response from the multilayer samples can be modeled by assuming that each individual layer of silver-decorated nanoparticles covered with a silica layer is equivalent to a thin film source of SHG signal. Within this approximation and because the thickness of each layer is identical, the amplitude of the elementary SHG field generated from each layer is the same. With this model, we can express the total SHG field as $E_{SHG} = C(1 + Nb)$, where E_{SHG} represents the total SHG field generated within a nanocomposite with N active layers. Here, C is the normalization constant representing the SHG contribution from the back side of the substrate^{39,40} and b is the contribution from one nanocomposite layer normalized to the response of the substrate. Note that to account for the possible phase differences in the elementary metal-dielectric sources, we allow b to be complex. The corresponding total intensity is given by $I_{SHG} = C^2|1 + Nb|^2$ and the measured SHG intensity averaged over all angles of incidence was fitted with this model as a function of the number of layers. The result (Fig. 4) shows excellent agreement with the experiment. The contribution from the thin film source manifested by parameter b

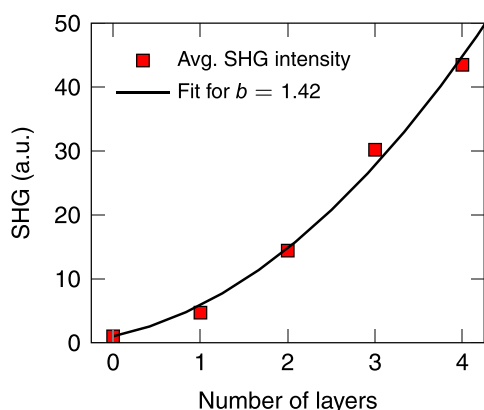


FIG. 4. Average SHG intensity as a function of the number of layers. Zero layers correspond to the substrate. The black line shows a fit with a model that separates contributions from the substrate and layers of the nanocomposite.

exceeds that from the substrate which is normalized to 1, consistent with the observations of Fig. 3(c). Corresponding value of the conversion efficiency of the second-order process was estimated to be of the order of 10^{-12} for the 4-layer sample, based on the experimental data. We also remark that the imaginary part of b is extremely small (1.1×10^{-5}), which is consistent with the fact that the SHG wavelength of 532 nm is significantly detuned from the plasmon resonance (see Fig. 3(b)). In principle and according to our model, the strength of the SHG signal could be boosted even more by depositing more active layers in the structure. In fact, with our thickest four-layer sample, we already observe 43-fold stronger SHG signal than the one measured for the substrate (see Fig. 4). In addition, the structures prepared for the present experiments are non-optimized. Therefore we expect that further development and optimization process allows the second-order response to be increased even more.

In conclusion, we have introduced a concept for the fabrication of silica-metal nanocomposites with controllable linear and nonlinear optical properties. Aerosol synthesis techniques were used to fabricate nanoparticle structures with enhanced nonlinear optical properties. The fabrication process allows creating ordered multilayer structures that preserve the shape of the plasmon resonance independently of the number of layers. We have further shown that separating multiple layers of decorated nanoparticles by silica results in an overall non-centrosymmetry that leads to second-harmonic generation that scales with the number of layers. Due to the flexibility of the used aerosol synthesis techniques, the material as well as the size of the carrier particles and the decorative nanodots can be varied to obtain nanocomposites with different optical responses (linear and nonlinear).

This work was supported by the Academy of Finland (136080 and 134980). M. Z. acknowledges the Wihuri Foundation for financial support. The authors thank Dr. Mari Honkanen (Department of Materials Science, Tampere University of Technology) for electron microscopy imaging, and Antti Rantamäki (Optoelectronics Research Centre, Tampere University of Technology) for preparing silica layers on the samples.

¹T. Okamoto, I. Yamaguchi, and T. Kobayashi, *Opt. Lett.* **25**, 372 (2000).

²J. J. Mock, D. R. Smith, and S. Schultz, *Nano Lett.* **3**, 485 (2003).

³A. Holden, *Photonics Nanostruct. Fundam. Appl.* **3**, 96 (2005).

⁴J. B. Pendry, *Phys. Rev. Lett.* **85**, 3966 (2000).

⁵M. A. Green and S. Pillai, *Nature Photonics* **6**, 130 (2012).

⁶A. Pors, A. V. Uskov, M. Willatzen, and I. E. Protsenko, *Opt. Commun.* **284**, 2226 (2011).

⁷J. J. Mock, S. J. Oldenburg, D. R. Smith, D. A. Schultz, and S. Schultz, *Nano Lett.* **2**, 465 (2002).

⁸J. R. Heath, *Phys. Rev. B* **40**, 9982 (1989).

⁹J. Krenn, G. Schider, W. Rechberger, B. Lamprecht, A. Leitner, F. Aussenegg, and J. Weeber, *Appl. Phys. Lett.* **77**, 3379 (2000).

¹⁰N. J. Halas, *Nano Lett.* **10**, 3816 (2010).

¹¹S. A. Maier, *Plasmonics: Fundamentals and Applications* (Springer, 2008).

¹²H. Husu, J. Mäkitalo, J. Laukkanen, M. Kuitinen, and M. Kauranen, *Opt. Express* **18**, 16601 (2010).

¹³J. E. Sipe and R. W. Boyd, *Phys. Rev. A* **46**, 1614 (1992).

¹⁴R. W. Boyd and J. E. Sipe, *J. Opt. Soc. Am. B* **11**, 297 (1994).

¹⁵C. K. Chen, A. R. B. de Castro, and Y. R. Shen, *Phys. Rev. Lett.* **46**, 145 (1981).

- ¹⁶H. Tuovinen, M. Kauranen, K. Jefimovs, P. Vahimaa, T. Vallius, J. Turunen, N.-V. Tkachenko, and H. Lemmetyinen, *J. Nonlinear Opt. Phys. Mater.* **11**, 421 (2002).
- ¹⁷S. Kujala, B. K. Canfield, M. Kauranen, Y. Svirko, and J. Turunen, *Phys. Rev. Lett.* **98**, 167403 (2007).
- ¹⁸R. Czaplicki, M. Zdanowicz, K. Koskinen, J. Laukkanen, M. Kuittinen, and M. Kauranen, *Opt. Express* **19**, 26866 (2011).
- ¹⁹M. W. Klein, C. Enkrich, M. Wegener, and S. Linden, *Science* **313**, 502 (2006).
- ²⁰F. Niesler, N. Feth, S. Linden, J. Niegemann, J. Gieseler, K. Busch, and M. Wegener, *Opt. Lett.* **34**, 1997 (2009).
- ²¹M. Hentschel, T. Utikal, H. Giessen, and M. Lippitz, *Nano Lett.* **12**, 3778 (2012).
- ²²G. Xu, M. Tazawa, P. Jin, and S. Nakao, *Appl. Phys. A* **80**, 1535 (2005).
- ²³J. Harra, J. Mäkitalo, R. Siikanen, M. Virkki, G. Genty, T. Kobayashi, M. Kauranen, and J. M. Mäkelä, *J. Nanopart. Res.* **14**, 870 (2012).
- ²⁴S. Linden, F. B. P. Niesler, J. Förstner, Y. Grynko, T. Meier, and M. Wegener, *Phys. Rev. Lett.* **109**, 015502 (2012).
- ²⁵D. M. Burland, R. D. Miller, and C. A. Walsh, *Chem. Rev.* **94**, 31 (1994).
- ²⁶S. I. Stupp, V. LeBonheur, K. Walker, L. S. Li, K. E. Huggins, M. Keser, and A. Amstutz, *Science* **276**, 384 (1997).
- ²⁷K. Chen, C. Durak, J. R. Hefflin, and H. D. Robinson, *Nano Lett.* **7**, 254 (2007).
- ²⁸A. Gurav, T. Kodas, T. Pluym, and Y. Xiong, *Aerosol Sci. Technol.* **19**, 411 (1993).
- ²⁹F. Krus, H. Fissan, and A. Peled, *J. Aerosol Sci.* **29**, 511 (1998).
- ³⁰G. A. Sotiriou, T. Sannomiya, A. Teleki, F. Krumeich, J. Vörös, and S. E. Pratsinis, *Adv. Funct. Mater.* **20**, 4250 (2010).
- ³¹A. M. Boies, P. Lei, S. Calder, and S. L. Girshick, *Nanotechnology* **22**, 315603 (2011).
- ³²G. A. Sotiriou, C. O. Blattmann, and S. E. Pratsinis, *Adv. Funct. Mater.* **23**, 34 (2013).
- ³³A. Binder, A. Heel, and G. Kasper, *Chem. Vap. Deposition* **13**, 48 (2007).
- ³⁴S. C. Wang and R. C. Flagan, *Aerosol Sci. Technol.* **13**, 230 (1990).
- ³⁵T. J. Krinke, K. Deppert, M. H. Magnusson, F. Schmidt, and H. Fissan, *J. Aerosol Sci.* **33**, 1341 (2002).
- ³⁶L. Mädler, A. Roessler, S. Pratsinis, T. Sahm, A. Gurlo, N. Barsan, and U. Weimar, *Sens. Actuators B* **114**, 283 (2006).
- ³⁷P. D. Maker, R. W. Terhune, M. Nisenoff, and C. M. Savage, *Phys. Rev. Lett.* **8**, 21 (1962).
- ³⁸J. Jerphagnon and S. K. Kurtz, *J. Appl. Phys.* **41**, 1667 (1970).
- ³⁹The literature values for the surface susceptibility of glass vary but are on the order of 10^{-22} m²/V, see Ref. 40.
- ⁴⁰F. J. Rodriguez, F. X. Wang, and M. Kauranen, *Opt. Express* **16**, 8704 (2008).